Supporting Information:

Electrochemical Detection of Extracellular Hydrogen Peroxide Released from RAW 264.7 Murine Macrophage Cells Based on Horseradish Peroxidase-Hydroxyapatite Nanohybrids

Chunyun Li[a], Hui Zhang[a]*, Ping Wu[a], Zhunan Gong[b], Guanglin Xu[b], Chenxin Cai[a]*

[a] Jiangsu Key Laboratory of New Power Batteries, Jiangsu Key Laboratory of Biofunctional Materials, Laboratory of Electrochemistry, College of Chemistry and Materials Science, Nanjing Normal University, Nanjing 210097, P. R. China.

[b] College of Life Science, Nanjing Normal University, Nanjing 210046, P. R. China.

* Corresponding author, E-mail: zhangh@njnu.edu.cn (H. Zhang), cxcai@njnu.edu.cn (C. Cai)

1. Synthesis of HAP Nanostructures.

The HAP nanostructures were synthesized by a chemical precipitation method according to the reported procedures with a minor modification.[1] The precipitation reaction was carried out following an idealized stoichiometric equation described as:[2] $6H_3PO_4 + 10Ca(OH)_2 = Ca_{10}(PO_4)_6(OH)_2$ (HAP) $+18H_2O$. Briefly, 300 mL of H_3PO_4 (0.3 M) was dropwisly added into a vigorously stirred aqueous solution of $Ca(OH)_2$ (0.25 M, 625 mL) with the temperature being controlled to 50~55 °C. After completion of H_3PO_4 addition, the pH value of the suspension was adjusted to 7.0 using 1 M ammonia. After aging for 12 h, HAP nanostructures were collected by filtering, washed thoroughly with double distilled water, and dried at 60 °C overnight. A powder was finally obtained and was readily used for subsequent characterization and enzyme immobilization.

2. XRD Patterns of the Prepared HAP Nanostructures.

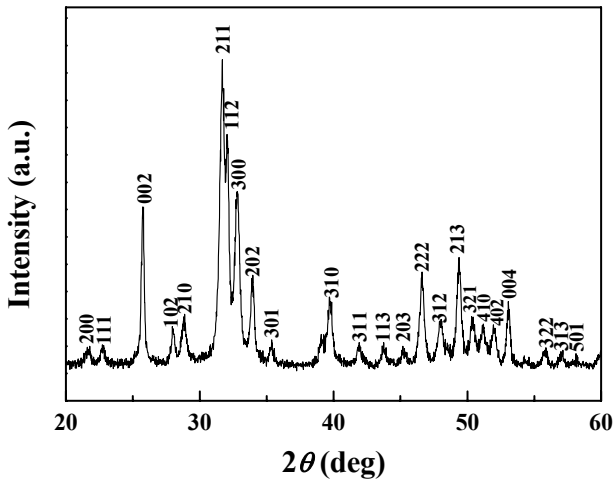

Figure S1. XRD patterns of as-synthesized HAP nanostructures.

The peaks at ca. 25.8, 31.7, 32.8, 34.0, 39.7, 46.6, 49.4, and 53.1° are observed and could be indexed to HAP (002), (211), (300), (202), (310), (222), (213), and (004) diffraction peaks, respectively.

3. IR Spectra of HAP Nanostructures and HRP-HAP Nanohybrids.

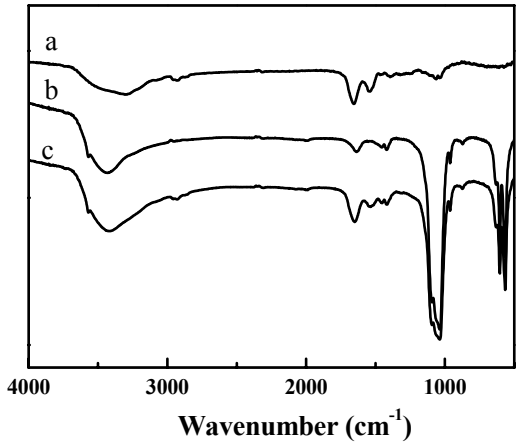

Figure S2. FT-IR spectra of HRP (a), HAP nanostructures (b), and HRP-HAP nanohybrids (c).

The IR spectrum of the prepared HAP nanostructures shows the characteristic stretching vibration modes of the P–O (~962 cm^{-1}, ~472 cm^{-1}, ~1035 cm^{-1}, and ~1091 cm^{-1}), and the bending vibration modes of O–P–O groups in PO_4^{3-} (~564 cm^{-1} and ~602 cm^{-1}), and the bending and the stretching vibrations of –OH groups (~1629 cm^{-1} and ~3569 cm^{-1}, respectively) (curve b). These features are identical with those reported previously for HAP,[3,4] demonstrating the successful preparation of HAP nanostructures. After the assembly of HRP, the major protein absorption bands due to the peptide group vibrations appear in the IR spectrum of HRP-HAP nanohybrids (curve c): amide I (~1655 cm^{-1}, the C=O stretching vibrations), and amide II (~1540 cm^{-1}, the N–H bending with contribution of the C–N stretching vibrations).[5-8] These characteristic absorption bands are very similar to those of the native protein (1654 and 1542 cm^{-1}) (curve a), indicating that HRP has been effectively assembled on the surface of HAP nanostructures, and moreover, the assembled HAP molecules can retain their native secondary conformation.

4. The Selectivity and Anti-interference Characteristics of the HRP-HaAP/GC Biosensor.

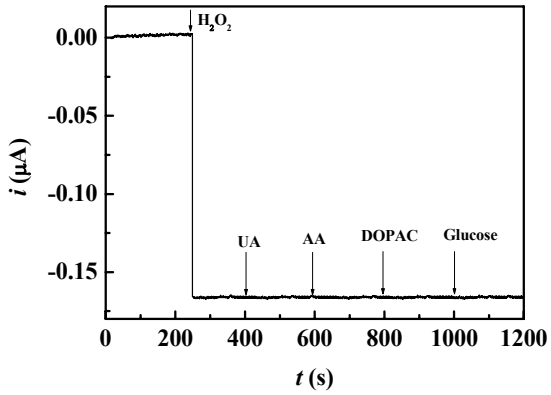

Figure S3. The selectivity profile of the electrode over interfering species of H_2O_2 (0.5 mM), UA (0.1 mM), AA (0.1 mM), DOPAC (0.1 mM), and glucose (5 mM) obtained at applied potential of –400 mV (versus SCE).

A well-defined H_2O_2 response is observed at the biosensor, whereas relevant physiological levels of UA (0.1 mM), AA (0.1 mM), DOPAC (0.1 mM), and glucose (5 mM) result in negligible signals.

5. DET Characteristics of HRP Assembled on HAP Nanostructures.

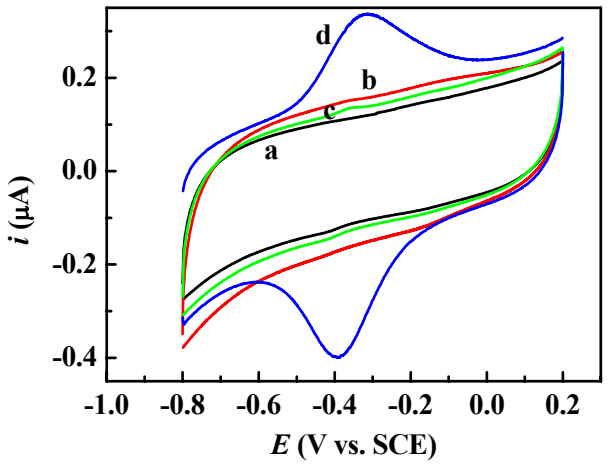

Figure S4. Cyclic voltammograms of the bare GC (a), HAP/GC (b), HRP/GC (c), and HRP-HAP/GC electrode (d) in N_2-saturated PBS (0.1 M, pH 7.4). The scanning rate was 100 mV s^{-1}.

No redox peaks are observed at the bare GC electrode in the potential range of interest (curve a), indicating that GC electrode itself is electroinactive. The cyclic voltammetric features of the HAP/GC electrode (curve b) are similar to those of the bare GC electrode except that the background currents have a slight enhancement, indicative of the increase in the apparent surface area of the electrode after modification with HAP. The cyclic voltammogram of the HRP/GC electrode shows a very small (almost undetectable) pair of redox peaks with the anodic (E_{pa}) and cathodic peak potential (E_{pc}) of ca. –360, and –410 mV, respectively (curve c). The height of the redox peaks decreases rapidly and disappears completely within a few scanning cycles (approx. 3–5 cycles). These results suggest that HRP cannot undergo the effective DET reaction at the surface of the bare GC electrode due to the redox center being deeply buried in the interior of the molecule. However, the cyclic voltammetric response of the HRP-HAP/GC electrode is characterized by a pair of well-defined and nearly symmetrical redox peaks with E_{pc} and E_{pa} of ca. –400 and –340 mV (at 100 mV s^{-1}), respectively (curve d). The formal potential, $E^{0'}$, which is defined as the average value of the E_{pa} and E_{pc}, is estimated to be –370 mV. This value is close to those previous reports for HRP trapped in polymer films, such as polyethylene glycol

(–370 mV)[9] and tributylmethylphosphonium chloride polymer (–377 ± 5 mV),[10] and also similar to that obtained by adsorbing HRP on the surface of TiO_2 (–350 mV).[11] Moreover, it is also similar to those of other heme proteins (enzymes) including hemoglobin[12] and myoglobin.[13] These results suggest that the pair of redox peaks presented in curve d can be assigned to the DET reaction (the conversion of Fe(III)/Fe(II) center) of HRP assembled on the surface of HAP nanostructures. The separation of peak potentials, ΔE_p, is 60 mV, indicating that HAP can facilitate the effective DET between HRP and the electrode surface in spite of the large molecular structure of HRP. These results also show that HRP assembled on the surface of HAP nanostructures can keep its natural structure. The conclusion is in good agreement with that obtained from UV-vis and IR spectra. Furthermore, the DET characteristics of HRP on the HAP surface is stable since the voltammetric features of the HRP-HAP/GC electrode remain almost unchangeable after the electrode was scanned continuously for a long time (~100 cycles, at 100 mV s^{-1}) in the potential range of experiment. In addition, no obvious change is detected after the electrode has been stored in PBS at 4 °C for one week. These characteristics are important when the electrode is further used as a biosensor for sensing substrates (such as H_2O_2, etc). The good stability of the HRP-HAP/GC electrode is due to that HRP-HAP nanohybrids can form a thin and uniform film on the surface of the GC electrode. This kind of film does not leak from the electrode surface and can stably adhere on the GC surface for a long time.

To further investigate the voltammetric characteristics of HRP assembled on the surface of HAP nanostructures, the effects of scan rates on the voltammetric response of the HRP-HAP/GC electrode were studied in detail. Almost equal cathodic and anodic peak heights can be observed at each scan rate, indicating that all electroactive ferrous HRP (HRP-Fe(II)), which was produced by reduction of ferric HRP (HRP-Fe(III)) on the forward scan, can be oxidized to HRP-Fe(III) on the reverse scan. Both the anodic and cathodic peak currents increase linearly with the scan rate up to at least 500 mV s^{-1}, suggesting that the redox process is confined to the surface of the electrode, also confirming that the assembled state of HRP is stable. Although the anodic and cathodic peak potentials shift slightly to

more positive and negative potentials, respectively, with the increase of the scan rate, the values of $E^{0'}$ (the average value is −(367 ± 5) mV in the scan rate range from 25 to 500 mV s^{-1}) are almost independent of the scan rates. From the dependence of ΔE_p on the scan rates, the apparent heterogeneous electron transfer rate constant, k_s, can be estimated to be (3.77 ± 0.78) s^{-1} using the method developed by Laviron for a surface-controlled electrochemical system.[14] This value is higher than (2.07 ± 0.56), 1.13, 1.15, and 1.1 s^{-1} obtained for HRP immobilized on carbon nanotube,[15] entrapped in DNA film,[16] immobilized on zinc oxide nanorods,[17] and confined in Nafion-cysteine film,[18] respectively, demonstrating again that HAP can effectively facilitate the DET of HRP.

REFERENCES

1 J. Hong, X. Qiu, J. Sun,M. Deng, X. Chen, and X. Jing, *Polymer*, 2004, **45**, 6699-6706.

2 H. J. Lee, H. W. Choi, K. J. Kim, and S. C. Lee, *Chem. Mater.*, 2006, **18**, 5111-5118.

3 M. C. Chang, W. H. Douglas and J. Tanaka, *J. Mater. Sci. Mater. Med.*, 2006, **17**, 387-396.

4 S. L. Michael, M. Shanthi, T. Ashok, A. Balasubramanian, A. Riyasdeen and M. A. Akbarsha, *Mater. Lett.*, 2009, **63**, 2123-2125.

5 A. Natalello, D. Ami, S. Brocca, M. Lotti and S. M. Doglia, *Biochem. J.*, 2005, **385**, 511-517.

6 (*a*) K. Niwa, M. Furukawa and K. Niki, *J. Electroanal. Chem.*, 1988, **245**, 275-285. (*b*) G. Irace, E. Bismuto, F. Savy and G. Colonna, *Arch. Biochem. Biophys.*, 1986, **244**, 459-469.

7 Q. Wang, W. Xu, P. Wu, H. Zhang, C. X. Cai and B. Zhao, *J. Phys. Chem. B*, 2010, **114**, 12754-12764..

8 W. L. Zhu, Y. Zhou and J. R. Zhang, *Talanta*, 2009, **80**, 224-230.

9 Y. Xu, W. L. Peng, X. J. Liu and G. X. Li, *Biosens. Bioelectron.*, 2004, **20**, 533-537.

10 T. Ferri, A. Poscia and R. Santucci, *Biosens. Bioelectron.*, 1998, **44**, 177-181.

11 Y. Zhang, P. L. He and N. F. Hu, *Electrochim. Acta*, 2004, **49**, 1981-1988.

12 H. Zhang, J. J. Xu and H. Y. Chen, *J. Phys. Chem. C*, 2007, **111**, 16564-16570.

13 (*a*) L. Meng, L. G. Yang, B. Zhou and C. X. Cai, *Nanotechnology*, 2009, **20**, 035502 (8pp). (*b*) Y. F. Lü, Y. J. Yin, P. Wu and C. X. Cai, *Acta Phys. –Chim. Sin.*, 2007, **23**, 5-11. (*c*) Y. J. Yin, H. Zhang, P. Wu, B. Zhou and C. X. Cai, *Nanotechnology*, 2010, **21**, 425504 (10pp).

14 E. Laviron, *J. Electroanal. Chem.*, 1979, **101**, 19-28.

15 Y. J. Yin, Y. F. Lü, P. Wu and C. X. Cai, *Sensors*, 2005, **5**, 220-234.

16 S. Q. Liu and H. X. Ju, *Anal. Biochem.*, 2002, **307**, 110-116.

17 B. X. Gu, C. X. Xu, G. P. Zhu, S. Q. Liu, L. Y. Chen, M. L. Wang and J. J. Zhu, *J. Phys. Chem. B*, 2009, **113**, 6553-6557.

18 J. Hong, A. A. Moosavi-Movahedi, H. Ghourchian, A. M. Rad and S. Rezaei-Zarchi, *Electrochim. Acta*, 2007, **52**, 6261-6267.